REPORT DOCUMENTATION PAGE

Form Approved OMB NO. 0704-0188

1. REPORT DATE (DD-MM-YYYY)	2. REPORT TYPE	3. DATES COVERED (From - To)
	New Reprint	-

4. TITLE AND SUBTITLE
Investigation of impurities in type-II InAs/GaSb superlattices via capacitance-voltage measurement

5a. CONTRACT NUMBER
W911NF-12-2-0009

5b. GRANT NUMBER

5c. PROGRAM ELEMENT NUMBER
622712

6. AUTHORS
A. M. Hoang, S. Bogdanov, A. Haddadi, P. R. Bijjam, B.-M. Nguyen, M. Razeghi, G. Chen

5d. PROJECT NUMBER

5e. TASK NUMBER

5f. WORK UNIT NUMBER

7. PERFORMING ORGANIZATION NAMES AND ADDRESSES
Northwestern University Evanston Campus
Office for Sponsored Research (OSR)
1801 Maple Ave., Suite 2410
Evanston, IL 60201 -3149

8. PERFORMING ORGANIZATION REPORT NUMBER

9. SPONSORING/MONITORING AGENCY NAME(S) AND ADDRESS(ES)
U.S. Army Research Office
P.O. Box 12211
Research Triangle Park, NC 27709-2211

10. SPONSOR/MONITOR'S ACRONYM(S)
ARO

11. SPONSOR/MONITOR'S REPORT NUMBER(S)
61310-EL.4

12. DISTRIBUTION AVAILIBILITY STATEMENT
Approved for public release; distribution is unlimited.

13. SUPPLEMENTARY NOTES
The views, opinions and/or findings contained in this report are those of the author(s) and should not contrued as an official Department of the Army position, policy or decision, unless so designated by other documentation.

14. ABSTRACT
Capacitance-voltage measurement was utilized to characterize impurities in the non-intentionally doped region of Type-II InAs/GaSb superlattice p-i-n photodiodes. Ionized carrier concentration versus temperature dependence revealed the presence of a kind of defects with activation energy below 6?meV and a total concentration of low 1015?cm?3. Correlation between defect characteristics and superlattice designs was studied. The defects exhibited a p-type behavior with decreasing activation energy as the InAs thickness increased from 7 to 11 monolayers, while

15. SUBJECT TERMS
Capacitance-voltage measurement impurities

16. SECURITY CLASSIFICATION OF:			17. LIMITATION OF ABSTRACT	15. NUMBER OF PAGES	19a. NAME OF RESPONSIBLE PERSON
a. REPORT	b. ABSTRACT	c. THIS PAGE			Manijeh Razeghi
UU	UU	UU	UU		19b. TELEPHONE NUMBER 847-/49-1725

Report Title

Investigation of impurities in type-II InAs/GaSb superlattices via capacitance-voltage measurement

ABSTRACT

Capacitance-voltage measurement was utilized to characterize impurities in the non-intentionally doped region of Type-II InAs/GaSb superlattice p-i-n photodiodes. Ionized carrier concentration versus temperature dependence revealed the presence of a kind of defects with activation energy below 6?meV and a total concentration of low 1015?cm?3. Correlation between defect characteristics and superlattice designs was studied. The defects exhibited a p-type behavior with decreasing activation energy as the InAs thickness increased from 7 to 11 monolayers, while maintaining the GaSb thickness of 7 monolayers. With 13 monolayers of InAs, the superlattice became n-type and the activation energy deviated from the p-type trend

REPORT DOCUMENTATION PAGE (SF298)
(Continuation Sheet)

Continuation for Block 13

ARO Report Number 61310.4-EL
Investigation of impurities in type-II InAs/GaSb s ...

Block 13: Supplementary Note

Approved for public release; distribution is unlimited.

Investigation of impurities in type-II InAs/GaSb superlattices via capacitance-voltage measurement

G. Chen,[1] A. M. Hoang,[1] S. Bogdanov,[1] A. Haddadi,[1] P. R. Bijjam,[1] B.-M. Nguyen,[2] and M. Razeghi[1,a)]

[1]*Center for Quantum Devices, Department of Electrical Engineering and Computer Science, Northwestern University, Evanston, Illinois 60208, USA*

[2]*Center for Integrated Nanotechnologies, Los Alamos National Laboratory, Los Alamos, New Mexico 87545, USA*

(Received 21 May 2013; accepted 25 June 2013; published online 17 July 2013)

Capacitance-voltage measurement was utilized to characterize impurities in the non-intentionally doped region of Type-II InAs/GaSb superlattice p-i-n photodiodes. Ionized carrier concentration versus temperature dependence revealed the presence of a kind of defects with activation energy below 6 meV and a total concentration of low 10^{15} cm^{-3}. Correlation between defect characteristics and superlattice designs was studied. The defects exhibited a p-type behavior with decreasing activation energy as the InAs thickness increased from 7 to 11 monolayers, while maintaining the GaSb thickness of 7 monolayers. With 13 monolayers of InAs, the superlattice became n-type and the activation energy deviated from the p-type trend. © *2013 AIP Publishing LLC*.
[http://dx.doi.org/10.1063/1.4813479]

After being proposed by Sai-Halasz *et al*. in the 1970s,[1] the short-period InAs/GaSb Type-II superlattices (T2SL) grown on GaSb substrate have been a promising alternative to the mercury cadmium telluride (MCT) system for infrared detection and imaging.[2] Because InAs and GaSb are closely lattice matched to each other, they offer great flexibility in designing devices for optical and electrical applications. In recent years, photodiodes with promising performance have been achieved because of the development of material quality,[3] innovative designs of device structure,[4–7] surface leakage current suppression technique,[8,9] and its unique band structure engineering capability, which leads to the great flexibility in engineering the band gap[10] and the suppression of Auger recombination,[11] diffusion,[12,13] and tunneling[14] current.

Despite this rapid development, there is still a discrepancy between the theoretical capabilities of this system and the experimental results of the minority carrier detectors because their electrical and optical performances are strongly related to their residual background carrier concentration. Since the residual background carrier concentration determines the minority carrier concentration and minority carrier lifetime, various studies have been done to understand its influence on device performance,[15–17] to find out correlations between the residual background carrier concentration and the growth conditions,[18,19] and to further optimize the growth condition for high purity T2SL detectors. Non-intentionally doped (nid) InAs is intrinsically n-type, while nid GaSb is intrinsically p-type,[20–22] which leads to complex nature of nid T2SL. It is generally believed that superlattice designs with thicker InAs layer tend to be intrinsically n-type, while those with thicker GaSb layer exhibit p-type behavior, and the carrier concentration is compensated by the n-doped and p-doped in InAs and GaSb, respectively. However, to date, there has not been any experimental evidence for the correlation between residual background carrier dynamics and superlattice designs. In this work, we utilized temperature dependent capacitance-voltage (C-V) measurement to extract the residual background carrier concentrations as well as the activation energy in nid T2SL, and experimentally established a quantitative dependence of these quantities on the superlattice designs.

C-V and Hall effect measurements are two standard characterization techniques of free carrier concentrations in semiconductor devices. The former technique is proven less challenging than the latter for measurements of thin film deposited on a conductive substrate.[23] High quality T2SLs are normally grown on conductive GaSb substrates that contribute significantly to the lateral transport of the sample. Hall measurement of T2SL requires either an extremely low temperature where carriers in GaSb become frozen,[24] or a complete substrate removal which makes the sample preparation complicated, or a high-quality surface passivation technique to minimize the effect from parasitic sidewall inversion.[25] C-V measurement enables a direct characterization of real device structures (i.e., a p-i-n photodiode) at different temperatures. The demonstration of C-V measurement for T2SL has been reported previously.[24] In particular, it has been shown that molecular beam epitaxy grown T2SL exhibits a background concentration of mid 10^{14} cm^{-3} at 77 K.[23]

To alter superlattice designs, we chose to vary the InAs layer thicknesses while maintaining the same GaSb layer thicknesses. This enables to span the cut-off wavelength of the superlattice from the mid-wavelength to long-wavelength infrared regimes as the superlattice band-gap is more sensitive to the InAs layer thickness than to the GaSb layer thickness. Four selected superlattice designs, denoted A, B, C, and D, consist of 7 monolayers (MLs) of GaSb and 7, 9, 11, and 13 MLs of InAs, respectively. All four samples were grown on GaSb (001) n-doped wafers by Intevac Modular Gen II molecular beam epitaxy system equipped with As/Sb valved cracker cells and Ga/In SUMO® cells.

a)Email: razeghi@eecs.northwestern.edu

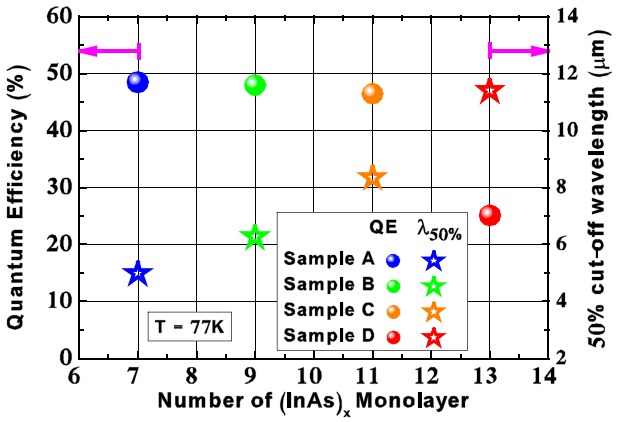

FIG. 1. The quantum efficiency at peak responsivity and 50% cut-off wavelength of different designs at 77 K.

They all have the same device structures, consisting of a 0.5 μm p^+-doped GaSb buffer, a 0.5 μm p-doped InAs/GaSb contact ($p\sim10^{18}\,cm^{-3}$), a 2 μm nid InAs/GaSb active region, a 0.5 μm n-doped InAs/GaSb contact ($n\sim10^{18}\,cm^{-3}$), and a 10 nm InAs n-type capping layer. All four samples were grown under the same growth condition as published in Refs. 26 and 27. Material characterization with high resolution x-ray diffraction showed that SL periods were consistent with the theoretical values. All samples were processed by the same processing technique as reported in Refs. 8, 9, and 12. The optical characteristics of all samples were first measured in a Janis Liquid Helium cryostat at 77 K. The analysis of each sample was performed on sets of diodes with sizes from 100×100 μm to 400×400 μm.

The quantum efficiency (QE) at peak responsivity, 50% cut-off wavelength, the calculated band gap based on the empirical tight binding model (ETBM),[10] and the measured band gap determined from the QE measurement of each sample are shown in Figure 1 and Table I. Samples A, B, and C have similar levels of QE despite different cut-off wavelengths, but sample D exhibits a significantly lower value. The discrepancy of the QE between sample D and the first three samples is due to different types of residual background of superlattice. Indeed, thicker InAs layer tends to result in n-type material, whereas thinner InAs layer makes the material p-type. Minority electrons have longer diffusion length than minority holes which results in higher QE of p-type material.[28] Since the nid 13 MLs InAs/7 MLs GaSb design has been proven to exhibit n-type semiconductor characteristic,[28] we can conclude that samples A, B, and C have residually p-type background, and sample D is n-type. This remark provides useful information for the C-V measurements since the C-V technique is incapable to determine the charge sign of carriers.

After the optical measurement, four best diodes with sizes from 250×250 μm to 400×400 μm from each sample were chosen for C-V measurement at temperatures ranging from 7 K to 120 K achieved by liquid helium cooling. The C-V measurement setup is described in Ref. 23. The reduced carrier concentration can be extracted from the slope of the linear fitting curve to the square of A/C versus the reverse bias voltage as explained by Eq. (1), where A is the diode area, C is the capacitance, V is the applied bias on the diode, q is the electron charge, and ε_o is the vacuum permittivity. Regardless of the residual carrier type in the nid region, the junction is heavily asymmetric due to the highly doped p^+ and n^+ contacts sandwiching the nid region (p^+n for intrinsically n-type nid region or n^+p for intrinsically p-type nid region), the measured reduced concentration is the ionized carrier concentration in the nid region. For relative permittivity, ε_r, we choose 15.4, a value between InAs and GaSb.[23] Figure 2 shows the reduced carrier concentration at temperature between 7 K and 120 K for a set of four diodes from each sample. The error bar for each data point was estimated from the error of the linear fit of the $(A/C)^2$ vs V slope,

$$N_{Red}=\frac{2}{q\varepsilon_r\varepsilon_0\dfrac{\partial\left(\dfrac{A^2}{C^2}\right)}{\partial V}}. \tag{1}$$

The temperature dependence of the reduced carrier concentration can be subdivided into three regions. Region I refers to the 1st kind of shallow level defects saturation regime. These defects have very small activation energy and are completely ionized even at very low temperature. Region II corresponds to the extrinsic region of the 2nd kind of shallow level defects. Regime III corresponds to the intrinsic regime. At low temperature, all samples stay in the Region I (7 K to 20 K for samples A and B and 7 K to 15 K for samples C and D), and their background concentrations do not change with temperature, which corresponds to the saturation of a type of shallow defects. This type of defects has a concentration around $1\times10^{14}\,cm^{-3}$ and activation energies well below the thermal energy at 7 K (0.6 meV). It is worth noting here that analysis has been done carefully to verify that the low constant concentration is not due to the limit of the system. At higher temperature, all four samples get into the Region II (20 K for samples A and B and 15 K for samples C and D) and their concentrations vary exponentially with the inverse temperature. The activation energies

TABLE I. Summary of design characteristics.

	Sample A	Sample B	Sample C	Sample D
Design	$(InAs)_7(GaSb)_7$	$(InAs)_9(GaSb)_7$	$(InAs)_{11}(GaSb)_7$	$(InAs)_{13}(GaSb)_7$
QE (%) at peak responsivity	48.5	48.0	46.5	25.2
Calculated E_g (meV)	252	194	149	114
Measured E_g (meV)	247 ± 5	199 ± 7	147 ± 3	108 ± 3
E_a (meV)	5.85	4.52	3.57	3.85
N_{Total} (cm^{-3})	1.23×10^{15}	1.17×10^{15}	1.10×10^{15}	9.88×10^{14}

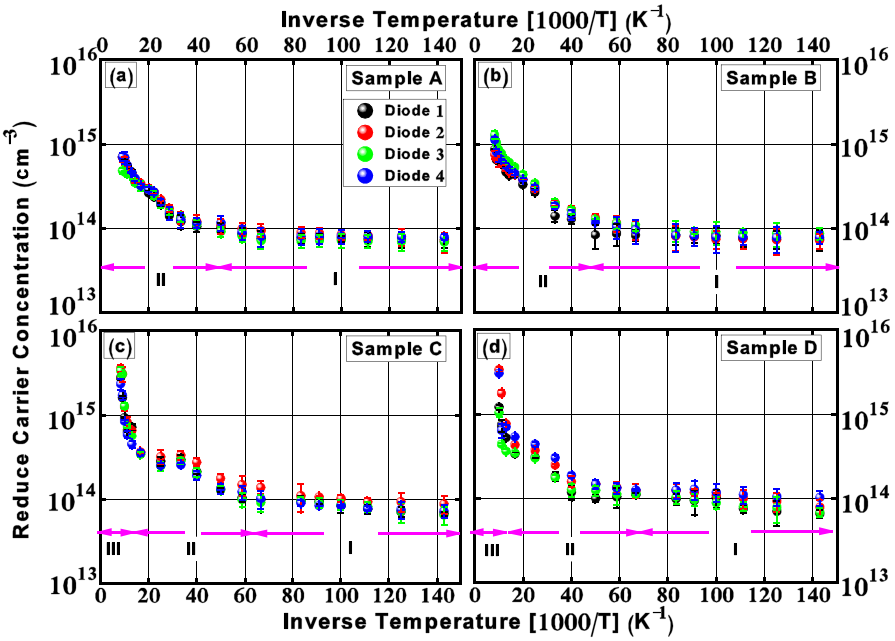

FIG. 2. The reduced carrier concentration versus inverse temperature. Region I is the saturation region of 1st kind of shallow level defects. Region II is the extrinsic region—the ionization region of 2nd kind of shallow level defects. Region III is the intrinsic region. Different colors stand for different diodes. Each sample has four different sizes diodes.

extracted from the slope of Region II of all four samples are reported in Table I. The extrinsic region of samples A and B extends up to 120 K and the intrinsic region is only observed in samples C and D. That is because samples C and D have relatively smaller band gap than samples A and B.

The total concentration of 2nd kind of shallow level defect (N_{Total}) can be extracted from the following equation, where *Ea* is the activation energy and *k* is the Boltzmann constant:

$$N_{Red} = N_{Total} \exp\left(-\frac{E_a}{kT}\right). \quad (2)$$

The values of N_{Total} of each sample are shown in Table I and Figure 3. This weak decrease in total concentration with the increase in InAs monolayer is due to the compensation of natively p-type GaSb by the n-type InAs of increasing thickness. Once the InAs layer is thick enough, type inversion happens. However, one should not expect the carrier concentration by the weight average of the donor and acceptor charges in the InAs and GaSb layer, respectively, because of the complicated convolution with the design-dependent activation energy as discussed below.

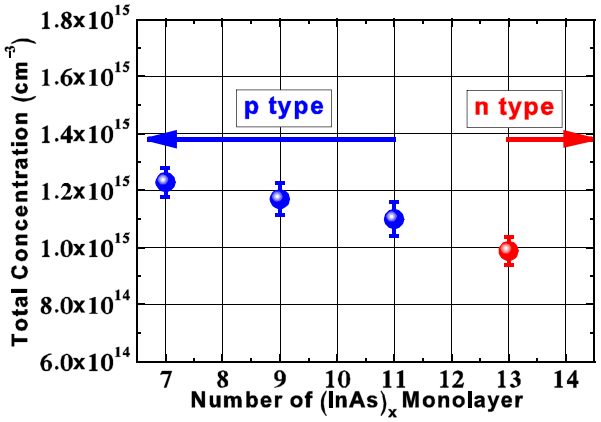

FIG. 3. The total concentration of 2nd kind of shallow level defect in different superlattice designs.

As shown in Figure 4, the activation energy of the 2nd kind of defect decreases as the InAs ML increases from 7 to 11 and then deviates from the trend at InAs ML = 13. This deviation could again be the result of background type inversion between sample D and the others. In the multiple-quantum well system, which is the case of type-II superlattice, the behavior of activation energy of impurity depends on the quantum well width, barrier width, and the barrier height. As the barrier width increases, wave function is forced to localize around the impurity ion because the penetration of wave function itself through the barrier becomes harder. This localization effect tends to increase the activation energy.[29] On the other hand, the thickness of the barrier in the superlattice is in the range that the wave functions penetration from adjacent wells cannot be neglected; these penetrated wave functions repulse each other, and thus increase the localization of the wave function around the impurity ion. However, increasing the thickness of barrier weakens this repulsive effect, which causes the wave function

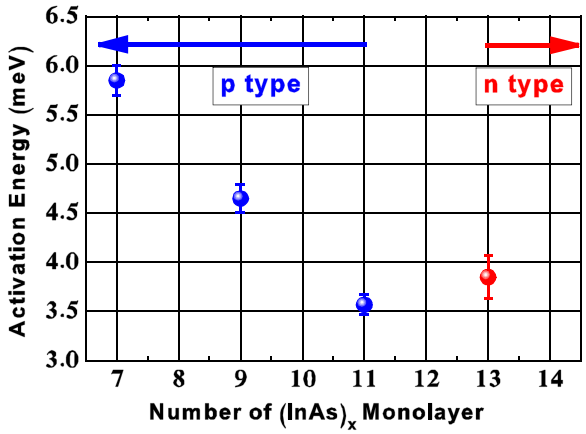

FIG. 4. The activation energy of the 2nd kind of defects decreases with the increase in number of InAs ML when the materials are p-type (InAs thickness from 7 to 11 MLs). The activation energy of the n-type material (13 MLs of InAs) deviates from the trend.

delocalization and results in the reduction in the activation energy.[30] The behavior of activation energy depends on the strength of these two competing effects. In the case of superlattice, the competition is expected to be more complicated due to the thin constituent layers and strong tunneling via the broken band gaps. However, experimental results suggest that the delocalization effect is stronger than the localization effect from the increment of the barrier and leads to the reduction of activation energy.

In summary, we show that if the GaSb thickness in an InAs/GaSb superlattice is kept constant at 7 MLs, there is a residual background type change when the MLs of InAs increases from 7 to 13. When the MLs of InAs is less than 11, the T2SL exhibits p-type semiconductor behavior; when the MLs of InAs is less than 13, the T2SL exhibits n-type semiconductor behavior. The dependence of the total concentration and activation energy of 2nd kind of shallow level defect on InAs layer thickness not only provides useful information to investigate the discrepancy between the theoretical limits and the experimental performance of devices based on this material system but also helps to further optimize the detector performance, such as utilize the type of nid InAs/GaSb superlattice to avoid doping the detector.

The authors acknowledge the support, interest, and encouragement of Dr. Meimei Tidrow, Dr. Fenner Milton, and Dr. Joseph Pellegrino from the U.S. Army Night Vision Laboratory, Dr. William Clark from U.S. Army Research Office, and Dr. Nibir Dhar from Defense Advanced Research Projects Agency. This material is based upon work supported by, or in part by, the U.S. Army Research Laboratory and the U.S. Army Research Office under cooperative Agreement No. W911NF-12-2-0009.

[1]H. Sakaki, L. L. Chang, G. A. Sai-Halasz, C. A. Chang, and L. Esaki, Solid State Commun. **26**, 589 (1978).
[2]A. Rogalski and P. Martyniuk, Infrared Phys. Technol. **48**, 39 (2006).
[3]B. M. Nguyen, G. Chen, M. A. Hoang, and M. Razeghi, IEEE J. Quantum Electron. **47**, 686 (2011).
[4]E. H. Aifer, J. G. Tischler, J. H. Warner, I. Vurgaftman, W. W. Bewley, J. R. Meyer, J. C. Kim, L. J. Whitman, C. L. Canedy, and E. M. Jackson, Appl. Phys. Lett. **89**, 053519 (2006).
[5]B.-M. Nguyen, D. Hoffman, P.-Y. Delaunay, E. K. Huang, M. Razeghi, and J. Pellegrino, Appl. Phys. Lett. **93**, 163502 (2008).
[6]J. B. Rodriguez, E. Plis, G. Bishop, Y. D. Sharma, H. Kim, L. R. Dawson, and S. Krishna, Appl. Phys. Lett. **91**, 043514 (2007).
[7]D. Z.-Y. Ting, C. J. Hill, A. Soibel, S. A. Keo, J. M. Mumolo, J. Nguyen, and S. D. Gunapala, Appl. Phys. Lett. **95**, 023508 (2009).
[8]G. Chen, B.-M. Nguyen, A. M. Hoang, E. K. Huang, S. R. Darvish, and M. Razeghi, Appl. Phys. Lett. **99**, 183503 (2011).
[9]G. Chen, E. K. Huang, A. M. Hoang, S. Bogdanov, S. R. Darvish, and M. Razeghi, Appl. Phys. Lett. **101**, 213501 (2012).
[10]Y. Wei and M. Razeghi, Phys. Rev. B **69**, 085316 (2004).
[11]H. Mohseni, V. I. Litvinov, and M. Razeghi, Phys. Rev. B **58**, 15378 (1998).
[12]A. Hood, D. Hoffman, B. M. Nguyen, P. Y. Delaunay, E. Michel, and M. Razeghi, Appl. Phys. Lett. **89**, 093506 (2006).
[13]S. A. Pour, E. K.-w. Huang, G. Chen, A. Haddadi, B.-M. Nguyen, and M. Razeghi, Appl. Phys. Lett. **98**, 143501 (2011).
[14]B.-M. Nguyen, D. Hoffman, P. Y. Delaunay, and M. Razeghi, Appl. Phys. Lett. **91**, 163511 (2007).
[15]E. da Silva, D. Hoffman, A. Hood, B. M. Nguyen, P. Y. Delaunay, and M. Razeghi, Appl. Phys. Lett. **89**, 243517 (2006).
[16]H. J. Haugan, S. Elhamri, F. Szmulowicz, B. Ullrich, G. J. Brown, and W. C. Michel, Appl. Phys. Lett. **92**, 071102 (2008).
[17]T. V. Chandrasekhar Rao, J. Antoszewski, L. Faraone, J. B. Rodriguez, E. Plis, and S. Krishna, Appl. Phys. Lett. **92**, 012121 (2008).
[18]H. J. Haugan, S. Elhamri, G. J. Brown, and W. C. Mitchel, J. Appl. Phys. **104**, 073111 (2008).
[19]C. Cervera, J. B. Rodriguez, J. P. Perez, H. Ait-Kaci, R. Chaghi, L. Konczewicz, S. Contreras, and P. Christol, J. Appl. Phys. **106**, 033709 (2009).
[20]D. J. Nicholas, M. Lee, B. Hamilton, and K. E. Singer, J. Cryst. Growth **81**, 298 (1987).
[21]Y. Wei, A. Hood, H. Yau, A. Gin, M. Razeghi, M. Z. Tidrow, and V. Natha, Appl. Phys. Lett. **86**, 233106 (2005).
[22]Chin-An Chang, R. Ludeke, L. L. Chang, and L. Esaki, Appl. Phys. Lett. **31**, 759 (1977).
[23]A. Hood, D. Hoffman, Y. Wei, F. Fuchs, and M. Razeghi, Appl. Phys. Lett. **88**, 052112 (2006).
[24]C. A. Hoffman, J. R. Meyer, E. R. Youngdale, F. J. Bartoli, and R. H. Miles, Appl. Phys. Lett. **63**, 2210 (1993).
[25]G. A. Umana-Membreno, B. Klein, H. Kala, J. Antoszewski, N. Gautam, M. N. Kutty, E. Plis, S. Krishna, and L. Faraone, Appl. Phys. Lett. **101**, 253515 (2012).
[26]Y. Wei, A. Gin, M. Razeghi, and G. J. Brown, Appl. Phys. Lett. **80**, 3262 (2002).
[27]B.-M. Nguyen, D. Hoffman, Y. Wei, P.-Y. Delaunay, A. Hood, and M. Razeghi, Appl. Phys. Lett. **90**, 231108 (2007).
[28]D. Hoffman, B.-M. Nguyen, P. Y. Delaunay, A. Hood, and M. Razeghi, Appl. Phys. Lett. **91**, 143507 (2007).
[29]G. Bastard, Phys. Rev. B **24**, 4714 (1981).
[30]S. Chaudhuri, Phys. Rev. B **28**, 4480 (1983).